Al-Nahrain Journal for Engineering Sciences **NJES** 26(1)14-23, 2023
http://doi.org/10.29194/NJES.26010014

Design and Performance Investigation of Intensity Modulation/Direct Detection Scheme for C- and O-band Point-to-Multipoint Optical Networks

Ali. S. Abed[1] and Raad. S. Fyath [2]

Authors affiliations:
1) Department of Computer Engineering, College of Engineering, Al-Nahrain University, Baghdad-Iraq.
st.ali.s.abed@ced.nahrainuniv.edu.iq

2) Department of Computer Engineering, College of Engineering, Al-Nahrain University, Baghdad-Iraq
raad.s.fyath@nahrainuniv.edu.iq

Abstract

The fifth generation (5G) and beyond mobile networks support increasing number of users with increasing bit rate per user. This has encouraged researchers to propose coherent digital subcarrier multiplexing (SCM) point-to-multipoint (P2MP) architectures to reduce the cost and complexity of optical transport networks, particularly in the metro aggregation scenario. However, coherent optical receiver is relatively cost and complex compared with a direct-detection (DD) counterpart due to the use of a synchronized local laser. This paper addresses design issues and performance investigation of intensity modulation/direct-detection (IM/DD) P2MP optical networks. P2MP architectures are designed using digital RF multisubcarrier (MSC) waveform embedded on the intensity of continuous-wave (CW) laser beside direct-detection scheme. The design covers covers Conventional-band (C-band) and Original-band (O-band) operation using a wavelength-division multiplexing (WDM) architecture. Further single- and double-polarization (SP and DP) versions are reported for each type of the networks. All the architectures are built in Optisystem version 15 environment and simulated for different network parameters, under the assumption of 25 Gbps per subcarrier data rate. The main performance measures are maximum route reach and bit rate-distance product (BDP). The simulation results indicate that DD networks can replaced the coherent counterpart when number of subcarriers per optical channel is 4. Further, the O-band P2MP networks offer high values of maximum reach and BDP than C-band counterparts.

Keywords: Point-to-Multipoint Optical Network; Intensity Modulation/Direct Detection; Digital Multisubcarrier P2MP; 5G and Beyond.

التحقيق في التصميم والأداء لتعديل الكثافة / مخطط الكشف المباشر للشبكات البصرية من نقطة إلى نقاط متعددة في النطاق C وO

علي سعدي عبد[1] و رعد سامي فياض[2]

الخلاصة:

يدعم الجيل الخامس (G5) وما بعده شبكات الهاتف المحمول عددًا متزايدًا من المستخدمين مع زيادة معدل البت لكل مستخدم. وقد شجع ذلك الباحثين على اقتراح معماريات تعدد إرسال فرعي رقمي متماسك (SCM) من نقطة إلى عدة نقاط (P2MP) لتقليل تكلفة وتعقيد شبكات النقل الضوئية ، لا سيما في سيناريو التجميع المترو. ومع ذلك ، فإن جهاز الاستقبال البصري المتماسك مكلف نسبيًا ويمكن للمستخدم الوصول إليه بعيدًا مقارنةً بنظير الاكتشاف المباشر (DD) بسبب استخدام ليزر محلي متزامن. تتناول هذه الورقة مشكلات التصميم وفحص الأداء لشبكات P2MP الضوئية لتعديل الشدة / الكشف المباشر (IM / DD). تم تصميم معماريات P2MP باستخدام شكل موجة ناقل رقمي متعدد الترددات (MSC) مدمج في شدة ليزر الموجة المستمرة (CW) بجانب مخطط الكشف المباشر. يغطي التصميم تشغيل النطاقين C و O باستخدام هندسة تعدد الإرسال بتقسيم الطول الموجي (WDM). تم الإبلاغ عن المزيد من إصدارات الاستقطاب الفردي والمزدوج (SP و DP) لكل نوع من أنواع الشبكات. تم إنشاء جميع البنى في بيئة Optisystem الإصدار ١٥ ومحاكاة لمعلمات الشبكة المختلفة ، بافتراض ٢٥ جيجابت في الثانية لكل معدل بيانات ناقل فرعي. مقاييس الأداء الرئيسية هي الحد الأقصى للوصول إلى المسار ومنتج مسافة معدل البت (BDP). تشير نتائج المحاكاة إلى أن شبكات DD يمكن أن تحل محل النظير المتماسك عندما يكون عدد الموجات الحاملة الفرعية لكل

قناة بصرية ٤. علاوة على ذلك ، توفر شبكات النطاق O-band P2MP قيمًا عالية للوصول الأقصى و BDP مقارنة بنظيراتها في النطاق C.

1. Introduction

Over the last years, the request for high-capacity networks has increased to support multiple deployment of broadband connectivity [1-3]. This is a growing landscape, that is now being addressed by the realization of fresher technologies such as fifth generation (5G) and beyond, which present access to user in higher than gigabit speeds [4-8]. Current telecommunication networks use Internet Protocol (IP) [9] for traffic between spoke (user location) and hub (data center location) [10]. The low-speed (spoke) is connected to high-speed (hub), and this topology is called point-to-multipoint (P2MP) scheme [11-13]. Digital RF multisubcarriers (MSC) scheme can support P2MP applications since it facilitates savings by eliminating intermediate aggregation routers/switches and associated transceivers [14-16].

Using coherent detection in the user- receiver side to deal with high data in P2MP has attracted interest in the recent years [17-19]. The scan of literature reveals that the proposed P2MP optical networks used coherent detection scheme. For example, an 8-subcarrier (SC) P2MP network operating with 4 Gbps bit rate per SC and SP 16-QAM was demonstrated for 24 km transmission distance using coherent detection by Ren et al. [20]. Welch et al. [21] demonstrated P2MP coherent transceivers for 16-SC SP 16-QAM network each with 25 Gbps per SC over a transmission distance of 25 km. Zhou et al. [22] demonstrated 3-SC coherent P2MP network with transmission distance of 25 km and using SP 4-, 8-, and 16-QAM formats; the SC data rate is 2.14, 3.22 and 4.3 Gbps, respectively. Recent research by Fan et al. [23] proposed low cost P2MP coherent architecture using PAM-4 modulator with 2 SCs, and 10 Gbps bit rate for each subcarrier with 10 km transmission distance.

The high-speed IM/DD optical networks offer the advantages of low cost, low-power consumption, and small receiver footprint [24,25]. Further, IM/DD scheme (i.e., noncoherent scheme) is strongly recommended for implementing these advanced interconnects over coherent schemes. The main characteristics of IM/DD schemes are firstly, intensity modulation can be applied efficiently using directly modulated laser (DML) [26-28]. Secondly, DD needs one single-end photodiode (PD) and one analog-to-digital converter (ADC) [29-31]. In contrast, coherent receiver requires complex hardware including local laser (to act as a local oscillator and should be synchronized with the transmitter laser), balanced PDs, and more than one ADC [32,33].

In this paper, SP and DP MSC-P2MP optical networks are proposed using IM/DD scheme. The proposed networks are then incorporated in wavelength-division multiplexing (WDM) architectures to support C- and O-band operation. The transmission performance of the network is investigated for different network parameters using Optisystem ver.15 software.

2. Design P2MP Optical Network

This section gives design guidelines for the P2MP network under investigation. The network uses digital RF SCM-WDM with IM/DD scheme and operates either in C-or O- band. The group-velocity dispersion (GVD) of a single-mode fiber (SMF) is about 17 and 0 ps/(nm.km) at 1550 nm (C-band network) and 1310 nm (O-band network), respectively. Therefore, a dispersion-compensation fiber (DCF) is inserted in the P2MP route to compensate the GVD of the SMF when C-band operation is considered. In contrast, no DCF is inserted in the P2MP route for O-band operation. Further, a digital signal processing (DSP) is used in each SC-optical receiver to extract the data information from the photocurrent to enhance the detection process for that receiver. The architecture of P2MP can be explained with the aid of the block diagram depicted in Fig. 1.

2.1. Transmitter Side

The transmitter side uses an RF subcarrier multiplexed/WDM transmitter unit. Here, continuous-wave (CW) semiconductor lasers are employed, with each laser acts as a source of an unmodulated channel optical carrier. Figure 2 illustrates the first RF subcarrier modulation subsystem implemented in the Optisystem environment. This subsystem consists of quadrature amplitude modulator (QAM) mapper acting as a sequence generator that produces two parallel M-ary symbol sequences from the binary data. The M-ary generates multilevel pulses according to the M-ary signal input. Two lowpass filters (LPFs) having a cosine roll-off frequency transfer function are used to shape the spectrum of both in-phase (I) and quadrature (Q) components. The RF subcarrier modulation is achieved using a QAM modulator.

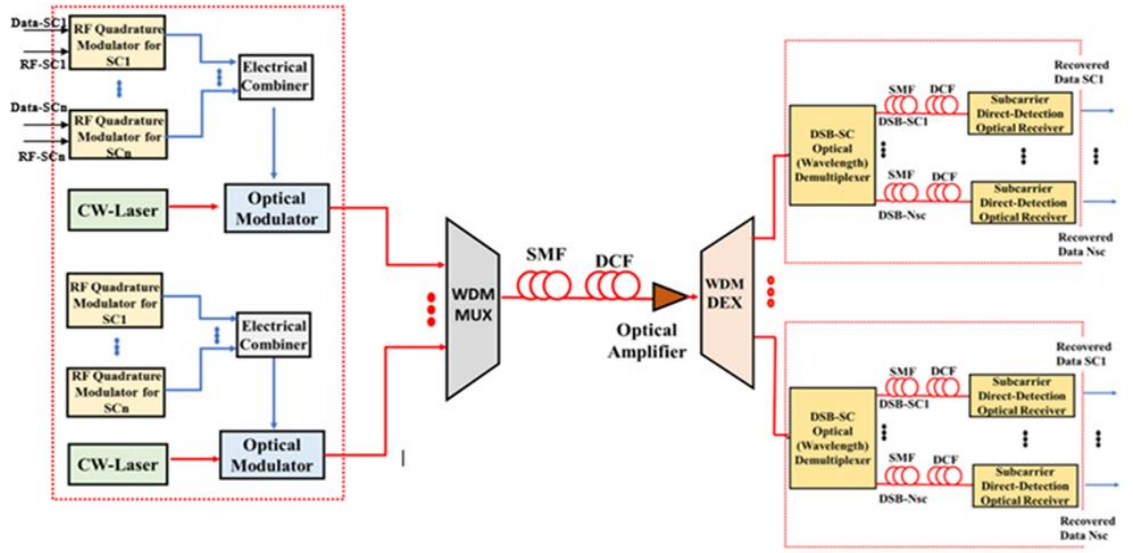

Figure. (1): Block diagram of the proposed P2MP wavelength-division multiplexing (WDM) network incorporating intensity modulation/direct-detection (IM/DD) scheme

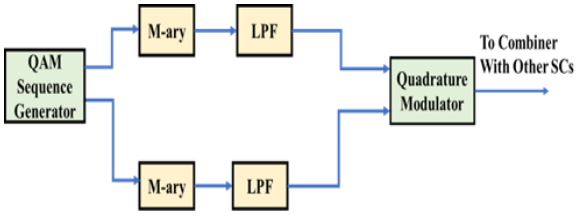

Figure (2): Single-subcarrier radio frequency (RF) QAM modulator used in the transmitter side of the P2MP architecture.

All the subcarriers modulation subsystems have identical configurations but each uses its own RF subcarrier as illustrated in Fig. 1. The RF subcarriers frequencies are separated by a subcarrier frequency spacing Δf_{sc} that prevents overlapping between neighboring subcarriers spectra. The MSC electrical signals (modulated RF signals) are combined using Nsc:1 electrical combiner where Nsc is the number of RF subcarriers. The combined signal is then applied to an optical Mach-Zender modulator (MZM) driven by a CW-laser. The generated optical signal goes to the WDM multiplexer which gather all optical channels (each channel has its own wavelength with channel spacing Δf_{ch}). The generated WDM signal is then launched to the fiber link. Table 1 lists suitable values for the optical channel frequency spacing required to design the related WDM networks.

2.2. Transmission Link

The transmission link of the P2MP network consists of a primary link (a common link that is shared by all RF subcarriers and all optical channels) and secondary links with each link provides connection to a specific subcarrier optical receiver (i.e., user end). In C-band operation, a DCF section is cascaded with each SMF section link to compensate its GVD. Also, an optical amplifire (OA) is inserted after the primary link to amplify the transmitted MSC-WDM signal. The gain of this amplifier is computed as [5]

$$G = \propto_{SMF} (L_{SMF1} + L_{SMF2}) + \propto_{DCF} (L_{DCF1} + L_{DCF2}) \ldots\ldots \quad (1)$$

where $\propto_{SMF}$ and $\propto_{DCF}$ is the loss parameter (dB/km) of the SMF and DCF, respectively, whose section lengths L_{SMF} and L_{DCF} measured in km. The subscripts 1 and 2 are used to distinguish the primary link (common link) from the secondary links that connected the WDM demultiplexer to the subcarrier optical receivers.

Table 1: Channel frequency spacing for different P2MP WDM networks.

Number of subcarriers	Optical channel frequency spacing Δf_{ch} (GHz)			
	16-QAM		64-QAM DP	
	SP	DP	SP	DP
4	150	75	100	50
8	250	150	200	100

2.3. Receiver Side

The first stage of the receiver side is a WDM demultiplexer (WDM DEMUX) that produces 1:N_{ch} output optical signals whose central optical frequencies match that of the transmitter channel frequencies. Each WDM demultiplexer output is connected to a proposed optical sideband demultiplexer (OSD), This demultiplexer is illustrated schematically in Fig. 3 and acts as a 1:($2N_{sc}$+1) wavelength splitter (i.e. wavelength decoder) that produces the lower-sideband (LSB) and upper-sideband (USB) of each optically modulated RF subcarrier beside the optical carrier component. This generated optical carrier is then applied to 1:Nsc optical splitter to support the N_{sc} optical receivers. The USB and LSB of each subcarrier are combined with one of the optical splitter outputs (optical carrier) to generate the intensity-modulated subcarrier optical signal corresponding to the SC under observation.

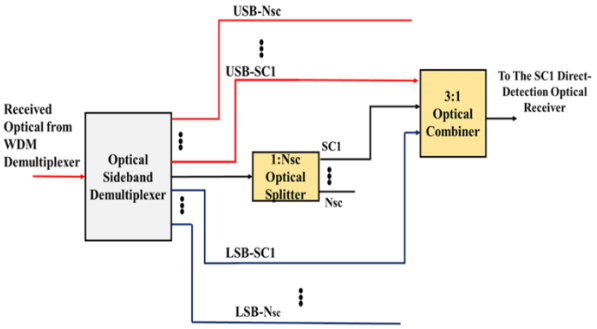

Figure (3): Proposed optical sideband demultiplexer

2.4. Primary Design Computation

This subsection presents design parameters computation related to a DD MSC-P2MP optical network. The network consists of multi-RF subcarriers embedded in a C-band optical carrier and the results can be extended to O-band version. Both SP and DP configurations are used for 16-QAM and 64-QAM subcarrier modulation formats and assuming DD scheme with 25 Gbps bit rate per subcarrier R_b. The simulation is performed with Optisystem software using the parameter values listed in Table 2. Design guideline is as follows:

i. In the 16-QAM format, the symbol rate Rs corresponds to SP- and DP-WDM channel is given, respectively, by [5]

$$(R_s)_{SP} = R_b/\mathrm{Log_2M} \quad (2)$$

$$(R_s)_{DP} = R_b/2\mathrm{Log_2M} \quad (3)$$

The symbol rate R_s for each subcarrier in DP network is 3.125 Gbaud (= 25 Gbps/(4×2)). This is to be compared with 6.25 Gbaud for the SP counterpart. The subcarrier frequency spacing is chosen according to

$$\Delta f_{sc} \geq 2B_{me} \quad (4)$$

Therefor 14 GHz and 8 GHz chosen for SP and DP networks, respectively. The first RF subcarrier frequency for the SP and the DP networks is 7 and 4 GHz, respectively. In addition, for the 64-QAM network, the symbol rate R_s for each subcarrier in DP system is 2.083 Gbaud (= 25 Gbps/ (6×2)). This is to compared with 4.166 Gbaud for the SP counterpart. Therefore, subcarrier spacing Δf_{sc} is chosen to be 10 GHz and 6 GHz for SP and DP networks, respectively. The first RF subcarrier frequency for the SP and the DP networks is 5 and 3 GHz, respectively the center channel frequency of C– and O-band in the WDM network is set to 193.1 THz (which corresponds to 1553.6 nm wavelength) and 228.5 THz (which corresponds to 1312.9 nm wavelength), respectively.

ii. The length of the transmission link between the transmitter and the ith subcarrier optical receiver L_i is given by

$$L_i = L_s + L_{bi} \quad (5)$$

where L_s is the lengh of the primary SMF connecting the transmitter to the WDM demultiplexer (common for all subcarrier) while L_{bi} is the length of the secondary SMF connecting the OSD output to the ith subcarrier receiver. If L_{bi} is assumed the same for all subcarriers, the P2MP network is then denoted by $(L_s + L_{bi})$ network.

iii. The length of the DCF section is chosen to yield a zero-average GVD over the fiber link

$$D_{SMF}L_{SMF} + D_{DCF}L_{DCF} = 0 \quad (6)$$

where D is the GVD, L is the fiber length, and the subscripts SMF and DCF are used to distinguish the two fiber types. From equ. (2)

$$L_{DCF} = -\frac{D_{SMF}L_{SMF}}{D_{DCF}} \quad (7)$$

iv. The maximum transmission reach is estimated as the maximum SMF route length that yields a bit error rate (BER) < BER_{th} for all the subcarriers. Here, BER_{th} denotes the threshold BER which is taken to 3.8×10^{-3} corresponding to 7% hard-decision (HD) forward error connecting (FEC) code.

Table 2: Parameters values used in the simulation.

Subsystem	Component	parameter	value
P2MP Transmitter	CW-Laser	Power	0 dBm
		Center frequency	193.1 THz @ C band
			228.5 THz @ O band
	RF-Quadrature Modulator	Modulation format	16-QAM
		Frequency spacing	14 GHz for SP
			8 GHz for DP
	optical modulator (MZ-Modulator)	Extinction ratio	30 dB
Transmission Link	Single-Mode-Fiber	Attenuation	0.2 dB/km @ C band
			0.35 dB/km @ O band
		Dispersion	17 ps/nm/km @ λ_{ref} = 1550 nm
			0 @ λ_{ref} = 1310 nm
		Dispersion slop	0.08 ps/nm²/km @ λ_{ref} = 1550 nm
			0.092 ps/nm²/km @ λ_{ref} = 1310 nm
		Effective area	80 μm²
		n2	26×10^{-21} m²/w
	Dispersion compensation fiber	Attenuation	0.5 dB/km @ λ_{ref} = 1550 nm
		Dispersion	-85 ps/nm/km @ λ_{ref} = 1550 nm
		Dispersion slop	-0.016 ps/nm²/km @ λ_{ref} = 1550 nm

		Effective area	23 μm²
		n2	26×10^{-21} m²/w
	Optical amplifier	Noise figure	4 dB
		Gain	6 dB @ C and O band
P2MP Receiver	Wavelength demultiplexer	Filter type	Gaussian
		Filter order	10
		Subcarrier spacing	14 GHz for SP
			8 GHz for DP
		Center frequency	193.1 THz
	Photodiode	Responsivity	1 A/W
		Dark current	10 nA
	RF-Quadrature demodulator	Modulation format	16-QAM
		frequency spacing	14 GHz for SP
			8 GHz for DP
	Digital signal processing (DSP)	Modulation format	16-QAM

3. Simulation Results

The transmission performance of the P2MP networks incorporating MSC/WDM multiplexing and DD scheme is investigated for different network parameters. Among these parameters are number of WDM channel N_{ch}, number of subcarriers per single-optical channel N_{sc}, modulation format (16-, 64-, and 128-QAM) and SP and DP in C- and O-band operation. For space limitation, sample of the obtained results are presented here which correspond to P2MP network designed with N_{ch} = 4 and N_{sc} = 8 when DP 16-QAM signaling is used.

3.1 Spectral Results of 8-SC 4-Ch P2MP-WDM Network

The P2MP network uses a WDM multiplexer at the transmitter side and WDM demultiplexer at the receiver side. The receiver side of each user also has an optical sideband demultiplexer (OSD) at its starting point that used to separate the spectra of upper and lower sidebands for each optically modulated RF subcarrier. These two side bands are combined with the optical carrier and forwarded to each user. Figures 4 and 5 illustrate the spectra of WDM optical channels that produced from WDM demultiplexer with channel spacing 150 GHz for C- and O-band networks, respectively. Each one of the four WDM demultiplexer outputs has its own OSD that separate optical channel to low- and upper-sidebands. The networks operate with DP 16-QAM signaling.

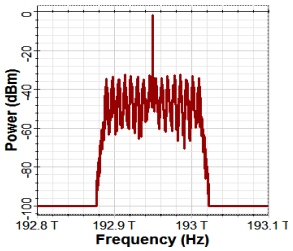

(a) Ch1.

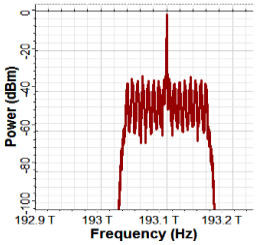

(b) Ch2.

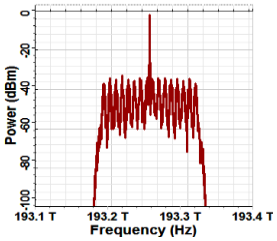

(c) Ch3.

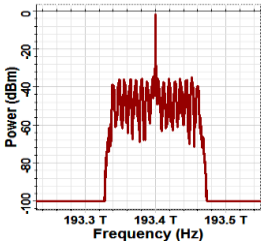

(d) Ch4.

Figure (4): Demultiplexed WDM channels for 8-SC 4-Ch P2MP WDM network operating in C band with DP 16-QAM signaling.

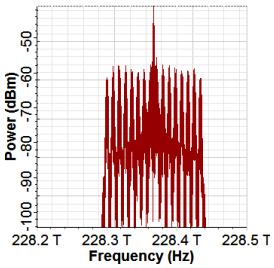

(a) Ch1.

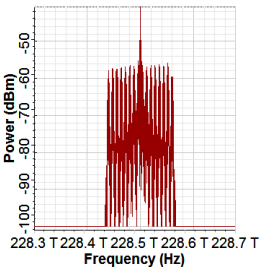

(b) Ch2.

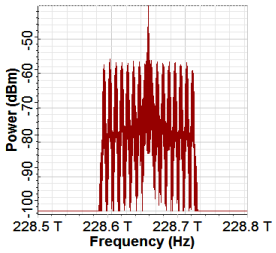

(c) Ch3.

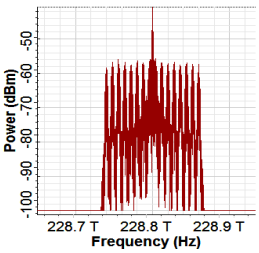

(d) Ch4.

Figure (5): Demultiplexed WDM channels for 8-SC 4-Ch P2MP WDM network operating in O band with DP 16-QAM signaling.

3.2 BER versus Transmission Distance for DD P2MP-WDM Network

Figures 6 and 7 represent the variation of BER of C- and O-band networks, respectively, with the transmission distance (L_s+ L_{bi}) for the last subcarrier (SC8) in each optical channel. The investigation reveals that SC8 is the first subcarrier that becomes out of service after number of km transmission. In

other word, SC8 is the first subcarrier that yields BERs>BER_{th} when transmission distance increases.

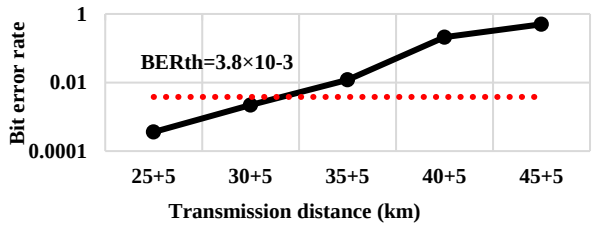

(a) SC8 of ch1.

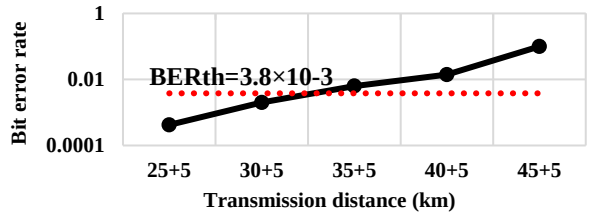

(b) SC8 of ch2.

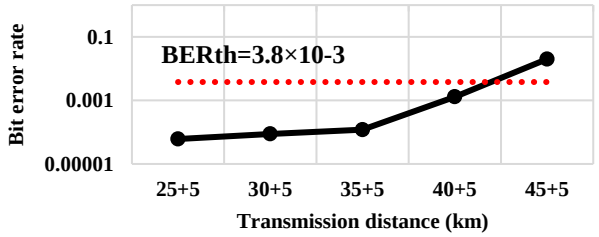

(c) SC8 of ch 3.

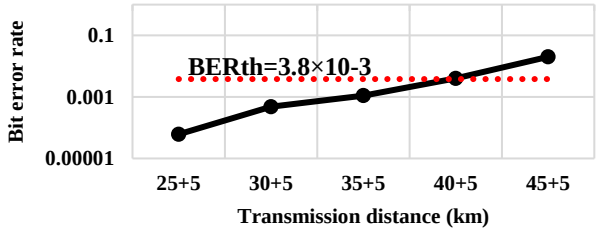

(d) Sc8 of ch 4.

Figure (6): Variation of BER for SC8 with transmission distance for each optical channel in 8-SC 4-Ch P2MP WDM network assuming C-band operation with DP 16-QAM signaling.

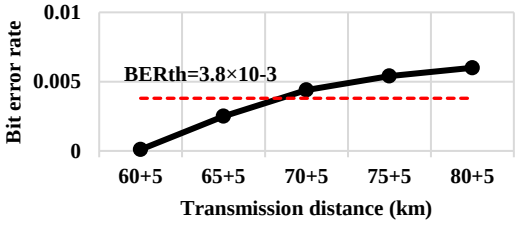

(a) SC8 of ch1.

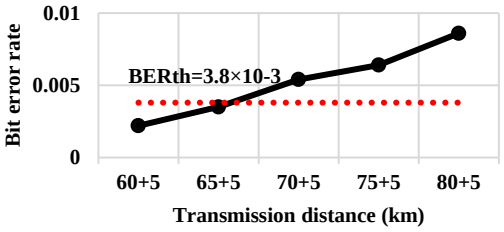

(b) SC8 of ch2.

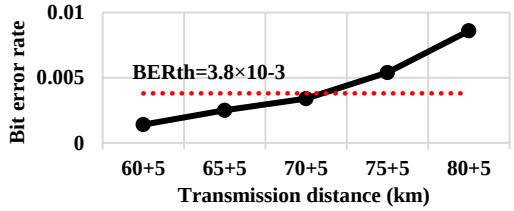

(c) SC8 of ch 3.

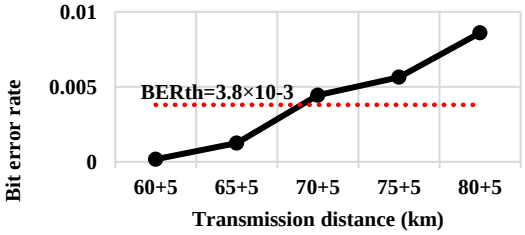

(d) Sc8 of ch 4.

Figure (7): Variation of BER of SC8 with transmission distance for each optical channel in 8-SC 4-Ch P2MP WDM network assuming O-band operation with DP 16-QAM signaling.

4. Total Bit Rate-Distance Product of C- and O-band P2MP Networks

It is clear that the total bit rate R_{bt} carried by the P2MP network increases linearly with the number of WDM channels N_{ch} and number of RF subcarriers per optical channel N_{sc}. This is true when each optical channel is modulated by the same number of RF subcarriers and each subcarrier carriers the same amount of bit rate R_b. Under these conditions, $R_{bt} = N_{sc}N_{ch}R_b$. However, the maximum reach L_{max} of P2MP network does not decreases linearly with increasing N_{sc} and N_{ch}. This leads to an unpredictable behavior describing the dependence of the total bit rate-distance product (BDP) on the number of WDM channels and number of RF subcarriers per each optical channel. The parameter BDP is a figure-of-merit (FoM) usually used to evaluate the transmission performance of optical networks. In this section, the parameters BDP is estimated for different P2MP network parameter using the relation BDP = $(N_{sc}N_{ch}R_b)L_{max}$. The results are listed in Tables 3 and 4 for C- and O-band networks, respectively. The results are presented for different values of N_{sc} and N_{ch}, and for different modulation formats assuming SP and DP architectures operating with R_b = 25Gbps. From the results reported in these two tables, one may deduce the maximum BDP obtained when the modulation format and the polarization type of the architecture are fixed as shown in Table 5 and Fig. 9. Investigation these results highlights the following facts:

i. The DP architecture offers higher maximum BDP compared with SP counterpart and this effect is more pronounce in O-band operation. For example, the 16-QAM C-band P2MP network offers 9/6.5=138.5% enhancement in BDP_{max} when the SP architecture is replaced by DP counterpart. This is to be compared with O-band operation where the enhancement is 80/14 = 571.4%.

ii. The O-band network offers higher BDP_{max} compared with C-band counterpart and this is true for any modulation format and polarization architecture. For example, the SP 16-QAM network has BDP_{max} = 6.5 and 14.0 Tbps.km for C- and O-band operation, respectively. These values are to be compared with 9.0 and 80.0 Tbps.km, respectively for DP 16-QAM networks.

TABLE 3: Maximum reach and total bit rate-distance product (BDP) for C-band P2MP network.
(a) Single-polarization network.

Modulation	Nch	Nsc per channel	L_{max}	BDP (Tbps.km)
16-QAM	1	4	65	6.5
		8	20	4.0
		12	8	2.4
		16	4	1.6
	4	4	60	6.0
		8	10	2.0
	8	4	40	4.0
		8	10	2.0
	16	4	28	2.8
64-QAM	1	4	52	5.2
		8	18	3.6
		12	8	2.4
		16	3	1.2
	4	4	50	5.0
		8	12	2.4
	8	4	35	3.5
		8	8	1.6
	16	4	25	2.5

TABLE 3: (Continued).
(b) Dual-polarization network.

Modulation	Nch	Nsc per channel	L_{max}	BDP (Tbps.km)
16-QAM	1	4	88	8.8
		8	45	9.0
		12	20	6.0
		16	12	4.8
	4	4	87	8.7
		8	35	7.0
	8	4	85	8.5
		8	20	4.0
	16	4	70	7.0
64-QAM	1	4	56	5.6
		8	25	5.0
		12	10	3.0
		16	4	1.6
	4	4	55	5.5
		8	25	5.0
	8	4	48	4.8
		8	12	2.4
	16	4	35	3.5

TABLE 4: Maximum reach and total bit rate-distance product (BDP) for O-band P2MP network.
(a) Single-polarization network.

Modulation	Nch	Nsc per channel	L_{max}	BDP (Tbps.km)
16-QAM	1	4	140	14.0
		8	30	6.0
		12	18	5.4
		16	7	2.8
	4	4	105	10.5
		8	18	3.6
	8	4	60	6.0
		8	10	2.0
	16	4	40	4.0
64-QAM	1	4	100	10.0
		8	20	4.0
		12	13	3.9
		16	5	2.0
	4	4	100	10.0
		8	25	5.0
	8	4	11	1.1
		8	10	2.0
128-QAM	1	4	40	4.0
		8	18	3.6
		12	10	3.0
		16	3	1.2

TABLE 4: (Continued).
(b) Dual-polarization network

Modulation	Nch	Nsc per channel	L_{max}	BDP (Tbps.km)
16-QAM	1	4	800	80.0
		8	300	60.0
		12	35	10.5
		16	25	10.0
	4	4	300	30.0
		8	70	14.0
	8	4	240	2.4
		8	40	8.0
	16	4	100	10.0
64-QAM	1	4	400	10.0
		8	120	2.4
		12	32	9.6
		16	25	10.0
	4	4	200	20.0
		8	50	10.0
	8	4	12	1.2
		8	11	1.1
128-QAM	1	4	200	20.0
		8	50	10.0
		12	30	9.0
		16	15	6.0

TABLE 5: Dependence of maximum BDP of P2MP network on modulation format and polarization architecture.
(a) C-band network

Modulation	Network	Maximum BDP	
		Values (Tbps.km)	Network parameter
16-QAM	SP	6.5	N_{ch} = 1 Nsc = 4
	DP	9.0	N_{ch} = 1 Nsc = 8

64-QAM	SP	5.2	N_{ch} = 1 Nsc = 4
	DP	5.6	N_{ch} = 1 Nsc = 4

TABLE 5: (continued).
(b) O-band network.

Modulation format	Network	Maximum BDP	
		Values (Tbps.km)	Network parameter
16-QAM	SP	14	N_{ch} = 1 Nsc = 4
	DP	80.0	N_{ch} = 1 Nsc = 4
64-QAM	SP	10.0	N_{ch} = 4 Nsc = 4
	DP	20.0	N_{ch} = 4 Nsc = 4
128-QAM	SP	4.0	N_{ch} = 1 Nsc = 4
	DP	20.0	N_{ch} = 1 Nsc = 4

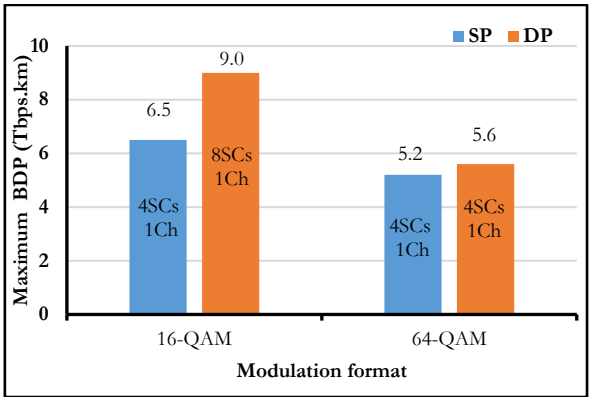

(a)

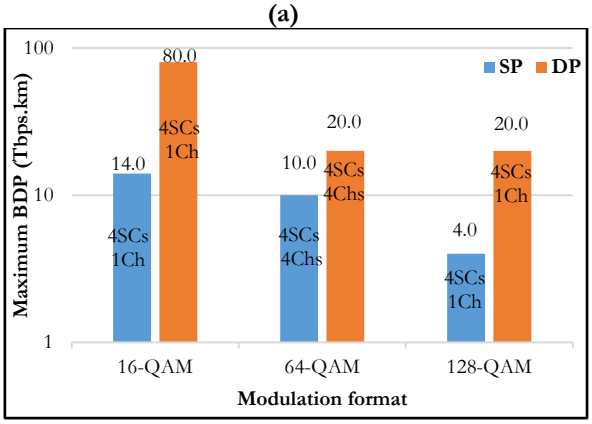

(b)

Figure (9): Variation of maximum bit rate-distance product (BDP_{max}) with modulation format and type of polarization. (a) C-band network. (b) O-band network.

5. Comparison with Related Work

Table 6 compares the transmission performance of optical networks reported in some recent related works with those obtained after simulation them using the methodology adopted in this paper. The optical networks covered by this comparison are related to a single-optical channel C-band P2P and P2MP operation with 25 Gbps bit rate per subcarrier. It is worth to mention here, that the related work uses coherent-detection scheme and supported by experimental results while the results obtained in this paper are obtained using simulation based on direct-detection scheme. The results in Table 6 reflect the following findings:

i. When Nsc = 4, the DD networks offer a maximum reach longer than the transmission distance used to implement the coherent-detection counterpart. For example, the DP QPSK and SP 16-QAM networks have been demonstrated over 50 and 35 km, respectively, using coherent-detection scheme. These are to be compared with Lmax = 85 and 65 km, respectively, when these networks are simulated using DD scheme

ii. When Nsc = 16, the DD network cannot support the transmission distance covered by the implemented coherent-detection counterpart. This network has been demonstrated over 35 km assuming SP 16-QAM while the simulated DD counterpart offers Lmax = 4 and 12 km for SP and DP version, respectively. Further simulation reveals that Lmax = 20 and 40 km when the P2MP network is designed with Nsc = 8 and using SP and DP architectures, respectively.

6. Conclusions

The transmission performance of IM/DD P2MP optical networks incorporating MSC/WDM technique has been investigated to support 5G and beyond services. Results have been reported for both C- and O-band operation assuming (16- and 64-QAM) and (16-, 64-, and 128-QAM) signaling, respectively. The main conclusions drawn from this paper are:

The maximum reach of optical route in C-band P2MP network is enhanced by using both DCF and receiver-side DSP for GVD compensating. The dual-polarization version of P2MP network offers longer route maximum reach (almost double) compared with single-polarization version. This is true for both C- and O-band operation. The O-band P2MP network supports longer maximum reach compared with C-band counterpart. For example, 16-SC 16-QAM network has L_{max} = 4 and 7 km for C- and O-band SP network, respectively. These are to be compared with 12 and 25 km, for C- and O-band DP networks, respectively. The DP architectures offer high maximum BDP compared with SP counterpart and this effect is more pronounced in O-band operation. For example, in C-band 16-QAM and N_{sc} = 16, BDP_{max} = 1.6 and 4.8 Tbps.km for SP and DP, respectively, while in O-band network, BDP_{max} = 2.8 and 10 Tbps.km for SP and DP, respectively.

Table 6: Comparison with related work.

Reference	Network parameters			Transmission distance	
	Modulation format	Number of subcarriers	Polarization architecture	Reference	This work
Zhang et al. [34] 2020 *	Q-PSK	4	DP	**50 km**	**85 km** (SP: 60 km)

Welch et al. [21] 2021	16-QAM	16	SP	**35 km** (25 km+10 km)	**4 km** (DP: 12 km)
Napoli et al. [10] 2022	16-QAM	4	SP	**55 km** (35 km+20 km)	**70 km** 60 km+5 km (DP: 82 km+5 km)

7. References

[1] K. Beman, M. Babri, G. Bi, and S. Oumtanaga," Multi- Spectrum bands allocation for time-varying traffic in the flexible optical network", *Int. J. Adv. Comput. Sci. Appl.*, vol. 7, no. 9, pp. 176–183, 2016.
https://doi.org/10.14569/ijacsa.2016.070925

[2] A. H. Ali, H. J. Alhamdane, and B. S. Hassen," Design analysis and performance evaluation of the WDM integration with CO-OFDM system for radio over fiber system", *Indones. J. Electr. Eng. Comput. Sci.*, vol. 15, no. 2, pp. 870–878, 2019.
https://doi.org/10.11591/ijeecs.v15.i2.pp870-878

[3] B. Hamza, W. Saad, I. Shayea , N. Ahmad, N. Mohamed, D. Nandi, and G. Gholampour, "Performance enhancement of SCM/WDM-ROF-XGPoN system for bidirectional transmission with square root module", *IEEE Access,* vol. 9, pp. 49487–49503, 2021,
https://doi.org/10.1109/ACCESS.2021.3065285

[4] S. Chen, J. Zhang, Y. Jin, and B. Ai," Wireless powered IoE for 6G: Massive access meets scalable cell-free massive MIMO", *China Commun.*, vol. 17, no. 12, pp. 92–109, 2020.
https://doi.org/10.23919/JCC.2020.12.007

[5] B. S. Zouneme, G. N. Anoh, and S. Oumtanaga," Minimization of spectrum fragmentation for improvement of the quality of service in multifiber elastic optical networks", *Int. J. Adv. Comput. Sci. Appl.,* vol. 11, no. 5, pp. 264–271, 2020.
https://doi.org/10.14569/IJACSA.2020.011053

[6] E. Hong, I. Lee, B. Shim, Y. Ko, S. Kim, S. Pack, K. Lee, S. Kim, J. Kim, Y. Shin, Y. Kim, and H. Jung, "6G R&D vision: requirements and candidate technologies*", J. Commun. Networks*, vol. 24, no. 2, pp. 232–245, 2022,
https://doi.org/10.23919/jcn.2022.000015

[7] D. U. Delgado, C. A. Gutierrez, and O. Caicedo, "5G and beyond: past, present and future of the mobile communications", *IEEE Lat. Am. Trans.,* vol. 19, no. 10, pp. 1702–1736, 2021.
https://doi.org/10.1109/TLA.2021.9477273

[8] C. Ranaweera, J. Kua, I. Dias, E. Wong, C. Lim, and A. Nirmalathas, "4G to 6G: Disruptions and drivers for optical access", *J. Opt. Commun. Netw.*, vol. 14, no. 2, pp. A143–A153, 2022.
https://doi.org/10.1364/JOCN.440798

[9] A. Tyagi," TCP/IP Protocol Suite", *Int. J. Sci. Res.Comput. Sci. Eng. Inf. Technol.*, Vol. 6, no. 4, pp. 59–71, 2020.
https://doi.org/10.32628/cseit206420

[10] A. Napole, J. Back, N. Swenson, W. Sande, J. Pedro, F. Masoud, A. Chase, C. Fludger, H. Sun, T. Chiang, A. Mathur, K. Wu, "Enabling router bypass and saving cost using point-to-multipoint transceivers for traffic aggregation", *Optical Fiber Communication Conference 2022 (OFC 2022)*, Paper no. W3F.5, pp. 4–6, 2022.
https://doi.org/10.1364/OFC.2022.W3F.5

[11] M. M. Hosseini, J. Pedro, N. Costa, A. Napoli, J. E. Prilepsky, and S. K. Turitsyn," Optimized physical design of metro aggregation networks using point to multipoint transceivers", *Optical Fiber Communication Conference 2022 (OFC 2022),* Paper no. W3F.2, pp. 3–5, 2022.
https://doi.org/10.1364/OFC.2022.W3F.2

[12] D. Borges, P. Montezuma, R. Dinis, and M. Beko," Massive mimo techniques for 5g and beyond opportunities and challenges", *Electron.,* vol. 10, no. 14, pp. 1–29, 2021
https://doi.org/10.3390/electronics10141667

[13] J. Back, P. Wright, J. Ambrose, A. Chase, M. Jary, F. Masoud, N. Sugden, G. Wardrop, A. Napoli, J. Pedro, M. A. Iqbal, A. Lord , D. Welch, "CAPEX savings enabled by point-to-multipoint coherent pluggable optics using digital subcarrier multiplexing in metro aggregation networks*", 2020 Eur. Conf. Opt. Commun. ECOC 2020,* no. 1, pp. 6–9, 2020.
https://doi.org/10.1109/ECOC48923.2020.9333233

[14] R. F. Chisab, and C. K. Shukla," Comparative study in performance for subcarrier mapping in uplink 4G-LTE under different channel cases", *Int. J. Adv. Comput. Sci. Appl. ((IJACSA),* vol. 5, no. 1, 2014.
https://doi.org/10.14569/IJACSA.2014.050107

[15] A. Naeem, S. Shafique, Z. Wadud, S. Ahmed, N. Safwan, and Z. Najam," Strategic planning towards automation of Fiber to The Home (FTTH) considering Optic Access Network (OAN) model", *Int. J. Adv. Comput. Sci. Appl.*, vol. 10, no. 9, pp. 234–244, 2019.
https://doi.org/10.14569/ijacsa.2019.0100930

[16] M. Iqbal, M. Ruiz, N. Costa, A. Napoli, J. Pedro, and L. Velasco," Dynamic and efficient point-to-point and point-to-multipoint communications by slicing the optical constellation", *Optical Fiber Communication Conference 2022 (OFC 2022),* paper no. Th2A.22 , pp. 2020–2022, 2022.
https://doi.org/10.1364/OFC.2022.Th2A.22

[17] N. Skorin-Kapov, F. J. M. Muro, M. V. B. Delgado, and P. P. Marino," Point-to-Multipoint coherent optics for re-thinking the optical transport: case study in 5g optical metro networks", *25th Int. Conf. Opt. Netw. Des. Model. ONDM 2021,* pp. 1–4, 2021.
https://doi.org/10.23919/ONDM51796.2021.9492393

[18] P. P. Marino, N. S. Kapov, M. V. Delgado, J. Back, and A. Napoli," On the benefits of point-to-multipoint coherent optics for multilayer capacity planning in ring networks with varying traffic profiles*", J. Opt. Commun. Netw.,* vol. 14, no. 5, pp. B30–B44, 2022.
https://doi.org/10.1364/JOCN.448123

[19] S. Mhatli, B. Nsiri, M. Jarajreh, B. Hammami, and R. Attia," Performance of window synchronisation in coherent optical ofdm system", *Int. J. Adv. Comput. Sci. Appl.,* vol. 5, no. 2, pp. 30–35, 2014.
https://doi.org/10.14569/ijacsa.2014.050205

[20 H. Ren, M. Fu, X. Zeng, Z. Zhai, Y. Fan, Q. Liu, L. Yi, W. Hu, and Q. Zhuge, "Joint power optimization of PTMP coherent architecture for improving link budget in downlink transmission", *2020 Asia Commun. Photonics Conf. ACP 2020 and Int. Conf. Inf. Photonics Opt. Commun. (IPOC 2020),* no. 2, pp. 2020–2022, 2020.
https://doi.org/10.1364/acpc.2020.m4a.316
[21] D. Welch et al.," Point-to-Multipoint optical networks using coherent digital subcarriers*", J. Light. Technol.,* vol. 39, no. 16, pp. 5232–5247, 2021.
https://doi.org/10.1109/JLT.2021.3097163
[22] Z. Zhou. "Multipoint-to-point data aggregation using a single receiver and frequency-multiplexed intensity-modulated ONUs",*OFC 2022*, no. Tu2G.4, pp. 4–6, 2022.
https://doi.org/10.48550/arXiv.2110.11865
[23] Y. Fan, M. Fu, X. Liu, Y. Xu, L. Yi, W. Hu, and Q. Zhuge, "Low-cost asymmetric point-to-multipoint coherent architecture for access networks", *Optical Fiber Communication Conference 2022 (OFC 2022),* Paper no. Th3E.6, pp. 6–8, 2022.
https://doi.org/10.1364/OFC.2022.Th3E.6
[24] H. Wang, J. Zhou , J. Wei, D. Guo, Y. Feng, W. Liu, C. Yu, D. Wang , and Z. Li, "Multi-Rate nyquist-SCM for C-band 100 Gbit/s signal over 50 km dispersion-uncompensated link*", J. Light. Technol.,* vol. 40, no. 7, pp. 1930–1936, 2022.
https://doi.org/10.1109/JLT.2021.3131603
[25] D. Plabst." Achievable rates for short-reach fiber-optic channels with direct detection", *J. Light. Technol.,* vol. 40, no. 12, pp. 3602-3613, 2022.
https://doi.org/10.1109/JLT.2022.3149574
[26] D. Tsonev, S. Videv, and H. Haas," Unlocking spectral efficiency in intensity modulation and direct detection systems", *IEEE J. Sel. Areas Commun.,* vol. 33, no. 9, pp. 1758–1770, 2015.
https://doi.org/10.1109/JSAC.2015.2432530
[27] D. Che , Y. Matsui , R. Schatz , R. Rodes, F. Khan, M. Kwakernaak, and T. Sudo "200-Gb/s Direct modulation of a 50-GHz Class Laser With Advanced Digital Modulations", *J. Light. Technol.*, vol. 39, no. 3, 2021
https://doi.org/10.1109/JLT.2020.3043374
[28] S. Rajalakshmi, and T. Shankar," Investigation of different modulation formats for extended reach NG-PON2 using RSOA", *Int. J. Adv. Comput. Sci. Appl.,* vol. 10, no. 12, pp. 142–149, 2019
https://doi.org/10.14569/ijacsa.2019.0101220
[29] J. Clement, H. Maestre, G. Torregrosa, and C. R. Pousa," Incoherent optical frequency-domain reflectometry based on homodyne electro-optic downconversion for fiber-optic sensor interrogation", *Sensors (Switzerland),* vol. 19, no. 9, 2019.
https://doi.org/10.3390/s19092075
[30] A. Chaaban, Z. Rezki, and M. S. Alouini, "On the capacity of intensity-modulation direct-detection gaussian optical wireless communication channels: a tutorial", *IEEE Commun. Surv. Tutorials*, vol. 24, no. 1, pp. 455–491, 2022.
https://doi.org/10.1109/COMST.2021.3120087
[31] T. Nakajima et al., "106-Gb/s PAM4 operation of directly modulated DFB lasers from 25 to 70oC for transmission over 2-km SMF in the CWDM range", *Opt. InfoBase Conf. Pap.,* vol. 40, no. 6, pp. 1815–1820, 2021.
https://doi.org/10.1364/ofc.2021.tu1d.4
[32] S. Sharma, D. Parkash, and S. Singh," Analysis and design of WDM optical OFDM system with coherent detection using different channel spacing", *Lect. Notes Electr. Eng.*, vol. 597, Springer Cham, pp. 365–376, 2020.
https://doi.org/10.1007/978-3-030-29407-6_27
[33] X. Li, M. O'Sullivan, Z. Xing, M. E. Mousa-Pasandi, and D. V. Plant," Asymmetric self-coherent detection based on mach-zehnder interferometers", *J. Light. Technol.,* vol. 40, no. 7, pp. 2023–2032, 2022.
https://doi.org/10.1109/JLT.2021.3135000
[34] J. Zhang, Z. Jia, H. Zhang, M. Xu, J. Zhu, and L. A. Campos, "Rate-flexible single-wavelength TFDM 100G coherent PON based on digital subcarrier multiplexing technology", *Opt. InfoBase Conf.,* vol. Part F174-, pp. 2020–2022, 2020.
https://doi.org/10.1364/OFC-2020-W1E